Preparation of Hydroxyapatite-Containing Coatings on Pure Titanium by Linearly Increasing the Voltage in the Pulsed Bipolar Microarc Oxidation Process

Chia-Jung Hu[*], *Jia-Rong Lu*

Department of Materials Engineering, Tatung University, 40 Chungshan N. Road, 3rd Sec., Taipei 104, Taiwan
[*]E-mail: cjhu@ttu.edu.tw

Highly adhered ceramic coatings containing hydroxyapatite (HA) on pure titanium are critical for clinical application. High power input in a microarc oxidation process is required to deposit coatings with crystalline HA. However, the high power input, either in potentiostatic or galvanostatic modes, leads to poor adhesion. Different voltage controls (constant or linear increase) used in bipolar pulse microarc oxidation (MAO) in aqueous solutions containing calcium acetate ($Ca(CH_3COO)_2 \cdot H_2O$) and calcium dihydrogen phosphate ($Ca(H_2PO_4)_2 \cdot H_2O$) were investigated in this study. The results indicated that a linearly increasing voltage improved the adhesion between the coating and the substrate, resulting in a more stable coefficient with lower friction and a more compact coating with excellent wear resistance. The predominant phase varied from anatase to rutile as the applied voltage increased. More rutile, $CaTiO_3$ and HA crystals in the coatings were achieved when the linearly increasing voltage reached 400 V in an HA-containing electrolyte. The analysis of bioactivity by using the WST-1 assay revealed that an HA-containing coating on pure titanium prepared in an ethanol-containing electrolyte is beneficial to bioactivity.

1. INTRODUCTION

Titanium and its alloys are suitable materials for application in orthopedic and dental implants because of their lower modulus, superior biocompatibility, and enhanced corrosion resistance compared with more conventional stainless steels and cobalt-based alloys [1]. Microarc oxidation (MAO) has been employed for modifying the surface of titanium and its alloys to produce porous, firmly adhered titania coatings containing Ca and P, improving the bioactivity of implants [2, 3].

Either the potentiostatic [4-6] or galvanostatic mode [7, 8] has been employed in most MAO processes. When a constant voltage is used in a potentiostatic MAO process, an initial upsurge of current and high power input (V^2/R) on the metallic surface of a sample accompanied by low electrical resistivity occurs at the initial stage [9]. The evolution of large amounts of oxygen on the workpiece surface at the early stage of a constant-voltage MAO process tends to cause the formation of pulverescent coatings or coatings with poor adhesion. Although a galvanostatic process can be used to avert this problem, substantially high voltage or power input (I^2R) is applied on the surface of a sample near the end of the MAO process under constant current conditions because the resistivity of the coating obviously increases as the coating thickness increases. According to Matthew, above a critical power, the microdischarges that occur throughout a film can penetrate the substrate and transform into powerful arcs, which may cause destructive effects such as an open discharge channel or thermal cracking of the film [10]. To prevent the aforementioned disadvantages, a linearly increasing voltage was applied in this study.

Applying an apatite-containing coating on titanium alloys benefits biocompatibility. In most studies, subsequent treatments of MAO coatings, such as chemical treatment [11, 12], hydrothermal treatment [13, 14], and simulated body fluid immersion [15, 16], were required to prepare apatite-containing coatings. However, few reports have adopted one approach for the MAO process to successfully synthesize a hydroxyapatite (HA)-based coating on pure titanium [17, 18]. To facilitate the formation of an HA-based coating, organic modifiers are often used as electrolyte additives for the morphology- and size-controlled synthesis of HA (e.g., citric acid [19], ethylenediamminetetraacetic acid (EDTA, $C_{10}H_{16}N_2O_8$) [20], glycerol [21], and ethanol [22]). This study involved preparing an hydroxyapatite coating on pure titanium by using one approach for the MAO process in which appropriate organic modifiers were added to the Ca/P-containing electrolyte to improve bioactivity. This approach was used to understand whether the addition of organic modifiers and a linearly increasing voltage are suitable for modifying the surface of an MAO coating formed in electrolyte-containing nano-HA.

2. EXPERIMENTAL PROCEDURE

Rectangular samples (with dimensions of 50 mm × 15 mm × 2 mm) composed of cp-titanium were used as working electrodes. The samples were mechanically polished using waterproof abrasive paper up to 1000 grit and then ultrasonically degreased in acetone and distilled water. The aqueous electrolyte used for MAO contained calcium acetate monohydrate ($Ca(CH_3COO)_2 \cdot H_2O$), monocalcium phosphate monohydrate ($Ca(H_2PO_4)_2 . H_2O$), NaOH, EDTA-2Na, HA, ethanol, and glycerol ($C_3H_8O_3$). The concentration of the electrolyte is shown in Table 1. The temperature of the electrolytic solution in a stainless steel container (counter electrode) was maintained below 10 °C by using a chiller during the MAO process. To maintain the suspension of the solid HA powder in the electrolytic solution, continuous stirring was required. A pulsed bipolar electrical source with a power of 12 kW was used for the experiment. The treatment was conducted by adopting a constant or linear increase in the applied voltage. The applied voltages for the anode were 250, 300, 350, and 400 V, and

that for the cathode was 150 V; the fixed electrical parameters were bipolar rectangular pulses with a frequency of 1000 Hz, a duty ratio of 0.3, and a treatment time of 15 min.

Table 1. The component of electrolyte.

Electrolyte	Composition and concentration						
	$Ca(CH_3COO)_2 \cdot H_2O$ (g/L)	$Ca(H_2PO_4)_2 \cdot H_2O$ (g/L)	NaOH (g/L)	EDTA-2Na (g/L)	HA (g/L)	Ethanol (vol. %)	$C_3H_8O_3$ (vol. %)
A	13.2	6.3	12	45	0	0	0
B	13.2	6.3	12	0	10	0	0
C	13.2	6.3	12	0	10	25	0
D	13.2	6.3	12	0	10	0	25

Note: HA: $Ca_{10}(PO_4)_6(OH)_2$; EDTA-2Na: $C_{10}H_{14}N_2Na_2O_8 \cdot 2H_2O$

The phase and microstructure of the coatings were evaluated using X-ray diffraction (D2 PHASER XRD) and scanning electron microscopy (JSM-6500F, JEOL), respectively. The composition of the surface layer was analyzed using an energy dispersive spectroscope (EDS) incorporated into the scanning electron microscopy. The thickness and arithmetic mean surface roughness (Ra) of the coating were measured using an eddy current coating measurement gage (Fisher Isoscope MP10-E) and a surface profilometer (Mitutoyo SJ-201), respectively. The friction coefficients were measured using a computer-controlled oscillating ball-on-disc tribometer (CSM TRN 01-05600) equipped with an Al_2O_3 ball 6 mm in diameter. Measurement was conducted at a linear speed of 7.8 cm/s, a track radius of 3 mm, and a load of 5 N. Furthermore, the bioactivity of the MAO coatings was evaluated using a WST-1 (4-[3-(4-lodophenyl)-2-(4-nitrophenyl)-2H-5-tetrazolio]-1,3-benzene disulfonate) assay.

3. RESULTS AND DISCUSSION

3.1. Effect of applied voltage modes on the MAO coatings

Fig. 1 shows the thickness of the MAO coatings treated in Electrolyte A at constant voltages and linearly increasing voltages. As expected, the thickness of the MAO coatings increased as the applied voltage increased from 250 V to 350 V, irrespective of a constant voltage mode or a linearly increasing voltage mode. The thickness of the MAO coating prepared at a constantly applied voltage then began to drop to 5.9 μm until 400 V because the local violent arc discharge during the MAO process at a constant voltage of 400 V caused the outer layer of the MAO coating to detach from the coating surface.
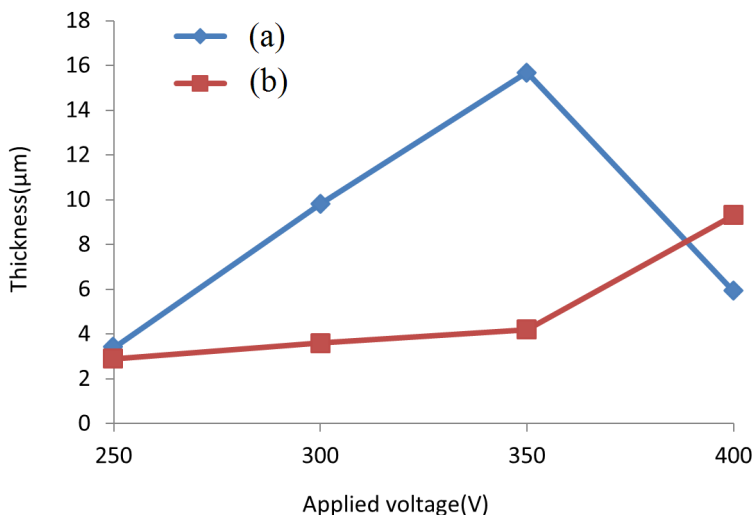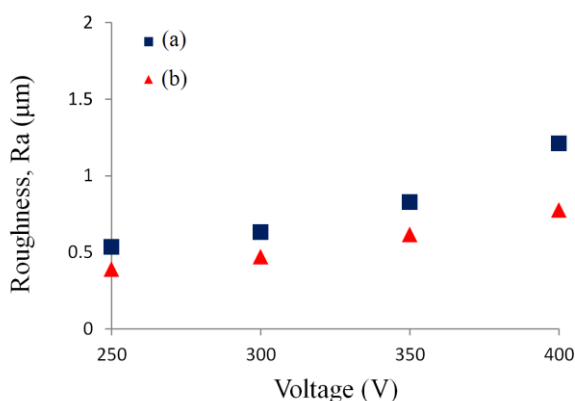
Figure 1. The thickness of the coatings on pure Ti after MAO treatment in Electrolyte A at (a) constant voltages and (b) linearly increasing voltages.
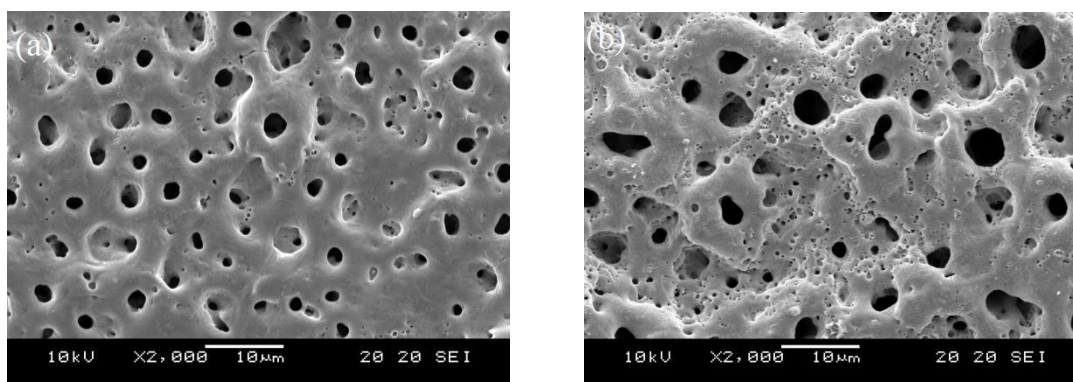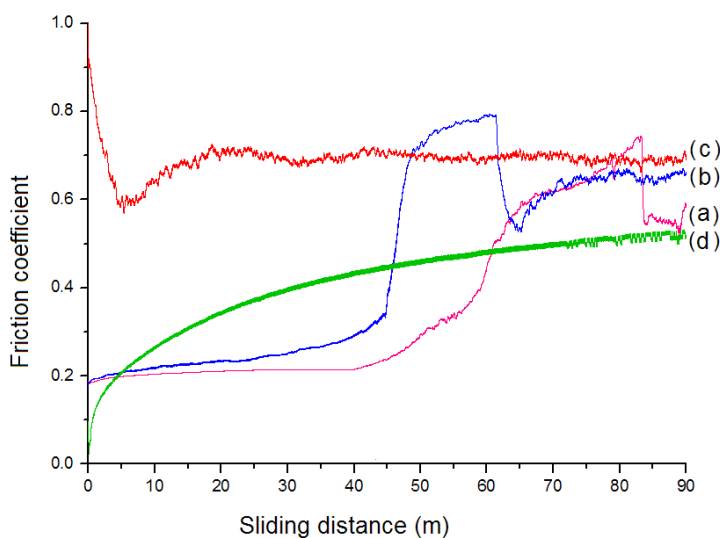

Figure 2. SEM morphologies of the coatings on pure Ti after MAO treatment in Electrolyte A at (a) a linearly increasing voltage to 400V (b) a constant voltage of 400V.

However, the thickness of the MAO coating prepared at a linearly increasing voltage to 400 V sharply increased to 9.3 μm. Compared with the smooth surface of the MAO coating prepared at a linearly increasing voltage (Fig. 2a), the coating prepared at a constant voltage of 400 V coarsened (Fig. 2b). Similarly, applying a constant voltage yielded a MAO coating with an Ra higher than that of the coating formed under a linearly increasing voltage, as shown in Fig. 3. Applying a constant voltage of 400 V also resulted in a substantially rougher coating because of the detachment of the outer layer, which is attributed to the initial upsurge of current and high power input (V^2/R) on the metallic surface of a sample [9], resulting a poor adhesion strength of the coating. As indicated in [23], the MAO coatings become more porous and crack with increasing voltage. According to the aforementioned results, a linearly increasing voltage process can improve the adhesion between the coating and substrate. Fig. 4 depicts friction coefficient plots of the coatings treated in Electrolyte A at a linearly increasing voltage to 350 V, a constant voltage of 350 V, a constant voltage of 400 V, and a linearly increasing voltage to 400 V. The friction coefficient of the coating treated at a linearly increasing

voltage to 350 V was lower than that of the coating treated at a constant voltage of 350 V. The friction coefficient of the coating treated at a linearly increasing voltage rapidly increased to ~0.6 after 60 m of sliding distance, whereas that of the coating treated at a constant voltage showed a steep rise to ~0.8 after 45 m of sliding distance; hence, the coating treated at a constant voltage deteriorated more quickly than the coating treated at a linearly increasing voltage did. For the coating prepared at a constant voltage of 400 V, the powdered debris created by the brittle porous outer layer of the MAO coating at the beginning of the 10-m sliding friction test caused the friction coefficient to be lower (Fig. 4 c). This unstable friction coefficient was observed after 10-m sliding because of the weak cohesive strength of the MAO coating. For the MAO sample prepared at a linearly increasing voltage to 400 V, the friction coefficients were lower and more stable (Fig. 4d), suggesting that a linearly increasing voltage improves the adhesion between the coating and substrate, resulting in excellent wear resistance.

Figure 3. The roughness of the coatings on pure Ti after MAO treatment in Electrolyte A at (a) constant voltages (■)and (b) linearly increasing voltages (▲) (0.37 of Ra for un-treated specimen).


Figure 4. Friction coefficient plots of the coatings on pure Ti after MAO treatment in Electrolyte A at (a) a linearly increasing voltage to 350V, (b) a constant voltage of 350 V, (c) a constant voltage of 400V, and (d) a linearly-increasing voltage to 400V.
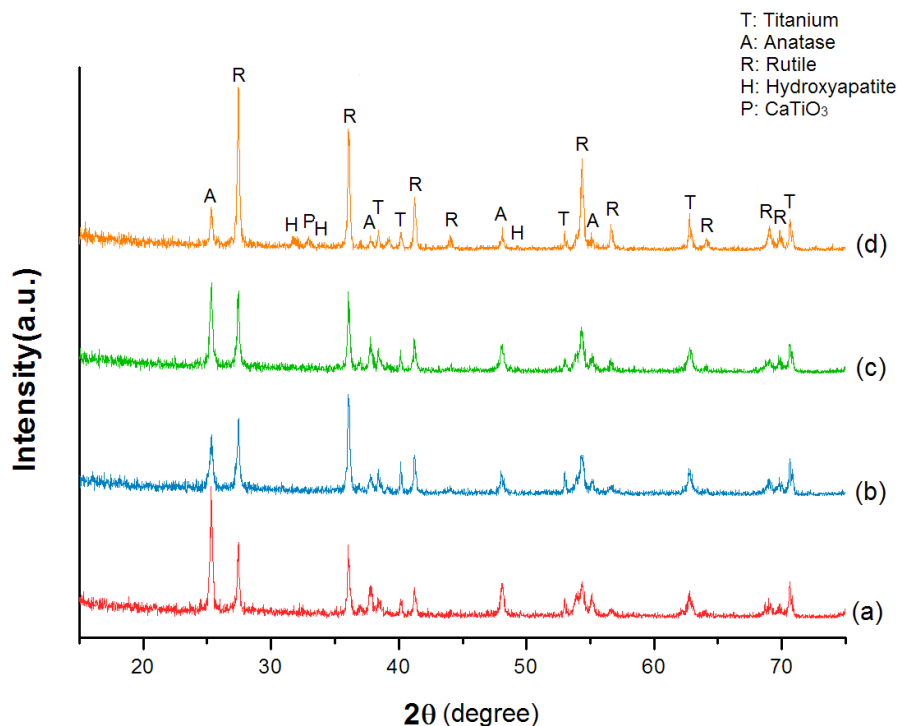
Figure 5. XRD patterns of surfaces of the coatings on pure Ti after MAO treatment at a linearly increasing voltage to (a) 350V in Electrolyte A, (b) 350V in Electrolyte B, (c) 400V in Electrolyte A, and (d) 400V in Electrolyte B.

3.2. Phase formation of the MAO coatings on pure titanium

The results of XRD revealed peaks of rutile and anatase in the coating formed in calcium acetate monohydrate/monocalcium phosphate monohydrate electrolytes at linearly increasing voltages (Fig. 5). The predominant phase varied from anatase to rutile as the applied voltage increased, irrespective of whether Electrolyte A or B was used. However, the rutile phase was more abundant in coatings prepared in Electrolyte B than in those prepared in Electrolyte A. HA crystals with small amounts of $CaTiO_3$ were observed in the coating prepared at 400 V in the HA-containing Electrolyte B; this suggested that the rutile phase is a high-temperature stable phase and that higher temperature generated by a higher applied voltage can promote the hydrolysis of monocalcium phosphate monohydrate and decomposition of calcium acetate monohydrate, generating more PO_4^{3-} and CO_3^{2-} ions. When both of these ions in the electrolyte adjacent to the anode reached a certain concentration, they reacted with the abundant Ca^+ ions to form HA precipitates according to the following reactions [24]:

$$10Ca^+ + 6PO_4^{3-} + 2OH^- \rightarrow Ca_{10}(PO_4)_6(OH)_2 \quad Ka = 6.3 \times 10^{116}$$
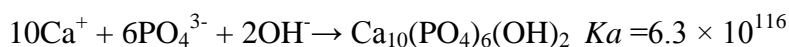
A similar mechanism was suggested by Han, who observed HA in coatings on Ti6Al4V prepared using MAO at a constant voltage of 450 V for 8–20 min in an aqueous electrolyte containing 0.02 M glycerophophate disodium and 0.2 M calcium acetate. Han indicated that the coatings consisted of two HA- and TiO_2-based layers; the HA-based outer layer contained small amounts of α-tricalcium phosphate and $CaCO_3$, and the TiO_2-based inner layer contained $CaTiO_3$ [18]. As shown in

Fig. 5c, HA crystals were not observed in the coatings formed at a linearly increasing voltage to 400 V in HA-free Electrolyte A. According to Han's suggestion [18], the aforementioned result may be attributed to the insufficient time or lower temperature of the electrolyte adjacent to the anode at a lower applied voltage. However, the HA powder in Electrolyte B facilitated the formation of HA crystals containing small amounts of $CaTiO_3$ on pure titanium (Fig. 5d). The TiO_2 then reacted with Ca^+ ions from the electrolyte to form $CaTiO_3$ at a high temperature generated by microarc discharge, as suggested by Han [18].
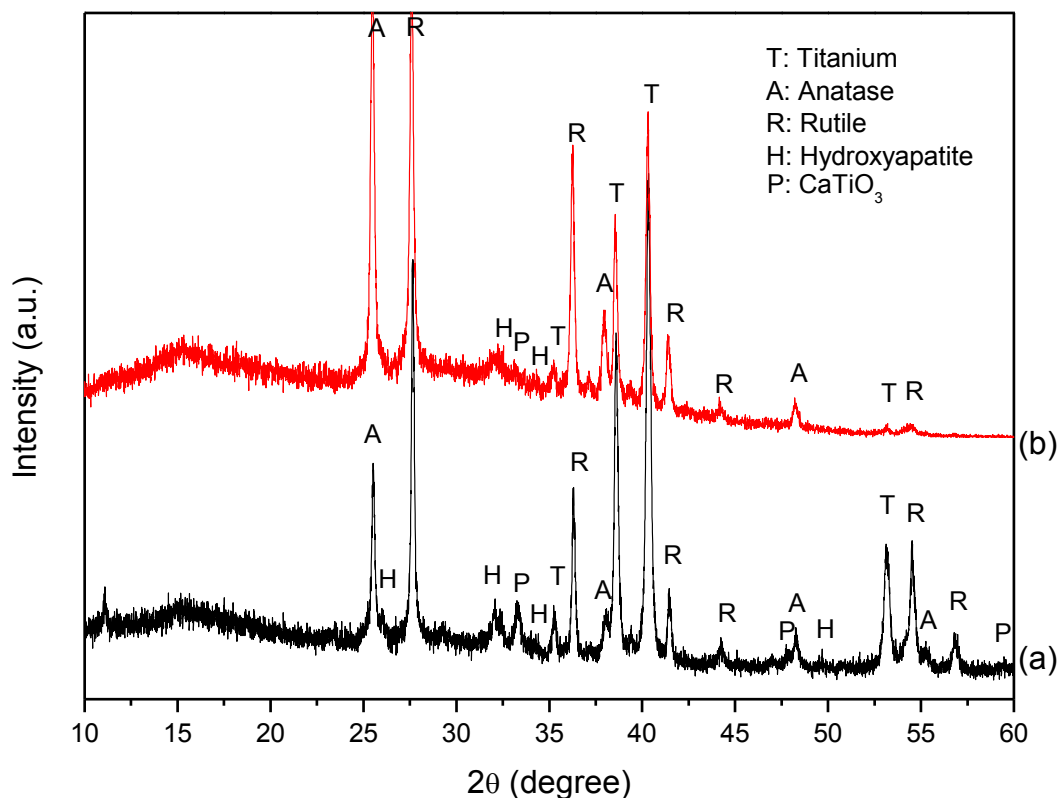
Figure 6. XRD patterns of the coatings on pure Ti after MAO treatment at a linearly increasing voltage to 400V in (a) Electrolyte C and (b) Electrolyte D.

As reported by Chen [25], the rutile-rich TiO_2 coating achieved superior biocompatibility and osteogenesis performance. Because more rutile and HA crystals formed on the coatings at a linearly increasing voltage to 400 V in HA-containing Electrolyte B, the HA suspensions that did not agglomerate in the electrolyte were achieved by adding organic modifiers to Electrolyte B, such as ethanol or glycerol, to facilitate the formation of HA crystals on a titania coating (Fig. 5d). Higher XRD peaks of HA and $CaTiO_3$ appeared in the coating formed in the ethanol-containing electrolyte (Electrolyte C) than that in the coating formed in the glycerol-containing electrolyte (Electrolyte D), as shown in Fig. 6. This suggested that the ethanol-containing electrolyte facilitated the formation of an HA-containing coating on pure titanium. As indicated in [26], adding ethanol to the electrolyte containing HA particles can retard the evolution of gas at the anode, which would otherwise obstruct

the attachment of HA particles. In addition, film containing $CaTiO_3$ can induce apatite to form on its surface, as indicated by Han and Hong et al. [27]. Fig. 6 shows a similar result with more HA crystals on the coating formed in the ethanol-containing electrolyte than on that formed in the glycerol-containing electrolyte. Furthermore, according to the EDS analysis of the coatings, Ca- and P-containing coatings were formed after MAO treatment in the Ca/P-containing electrolytes, namely Electrolytes A, B, C, and D, at a linearly increasing voltage to 400 V. The HA crystals incorporated onto the surface of the coating formed in the ethanol/HA-containing electrolyte (Electrolyte C) were more uniformly distributed than those on the coatings formed in the other electrolytes, suggesting that ethanol was the most effective organic modifier used.
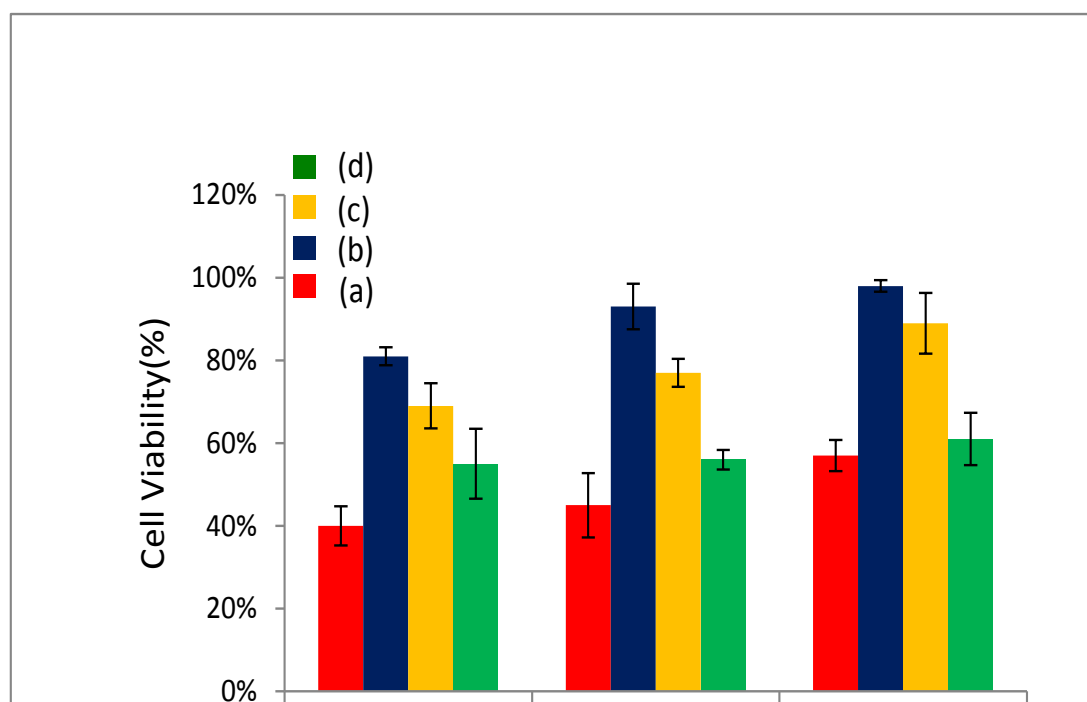
Figure 7. Cell viability measured by WST-1 assay after culturing for 1, 3, and 5 days on (a) pure Ti substrate, (b) Ti substrate after MAO treatment in Electrolyte C at a linearly increasing voltage to 400V, (c) Ti substrate after MAO treatment in Electrolyte D at a linearly increasing voltage to 400V and (d) Ti substrate after MAO treatment in Electrolyte A at a constant voltage of 400V.

3.3. Bioactivity of the MAO coatings on pure titanium

The cell viability of the samples was measured using a WST-1 assay after the cells were cultured for 1, 3, and 5 days, as shown in Fig. 7. The cell growth on the sample after MAO treatment in HA/ethanol-containing Electrolyte C was markedly higher than that on the sample formed in Electrolyte D and the noncoated titanium sample. XRD patterns of the coatings (Fig. 6) confirmed that the electrolyte containing ethanol (Electrolyte C) possessed more HA crystals, $CaTiO_3$, and rutile phases than the electrolyte containing glycerol (Electrolyte D). As indicated in [25], the rutile-rich TiO_2 coating achieved better biocompatibility, osteogenesis performance. Moreover, $CaTiO_3$

combined with calcium phosphate seems to be the key structural factor for MAO-formed titania-based films to be of bioactivity [2]. The formation of HA directly on the coating surface by MAO technique can greatly enhance the surface bioactivity [28, 29]. Therefore, the more HA, CaTiO$_3$, and rutile phases were incorporated into the coating, the higher the bioactivity of the coating was. The coating formed through MAO treatment at a linearly increasing voltage to 400 V in the ethanol/HA-containing electrolyte exhibited superior bioactivity.

4. CONCLUSION

An HA-containing oxide layer on pure titanium was successfully synthesized using one approach for a bipolar pulsed MAO process in an electrolyte containing nano-HA, calcium salts, and phosphates at a linearly increasing voltage to 400 V. Compared with the detachment of the outer layer in the MAO coating prepared at a constant voltage of 400 V, a linearly increasing voltage improved the adhesion between the coating and the substrate, resulting in excellent wear resistance. In addition, adding ethanol to the electrolyte facilitated the formation of an HA-containing coating on pure titanium, resulting in favorable bioactivity.

References

1. M. Long and H.J. Rack, *Biomaterials*, 19 (1998) 1621
2. Y. Han, S.-H. Hong and K. Xu, *Surf. Coat. Tech.*, 168 (2003) 249
3. D. Wei, Y. Zhou, D. Jia and Y. Wang, *Surf. Coat. Tech.*, 201 (2007) 8723
4. Z.Q. Yao, Y. Ivanisenko, T. Diemant, A. Caron, A. Chuvilin, J.Z. Jiang, R.Z. Valiev, M. Qi and H.-J. Fecht, *Acta Biomater.*, 6 (2010) 2816
5. Y. Yan, J. Sun, Y. Han, D. Li and K. Cui, *Surf. Coat. Tech.*, 205 (2010) 1702
6. M. M. Dicu, M. Abrudeanu, S. Moga, D. Negrea, V. Andrei and C. Ducu, *J. Optoelectron. Adv. Mater.*, 14 (1-2) (2012) 125
7. J.-Z. Chen, Y.-L. Shi, L. Wang, F.-Y. Yan and F.-Q. Zhang, *Mater. Lett.*, 60 (2006) 2538
8. K. Venkateswarlu, N. Rameshbabu, D. Sreekanth, A.C. Bose, V. Muthupandi, N.K. Babu and S. Subramanian, *Appl. Surf. Sci.*, 258 (2012) 6853
9. C.-J. Hu, J.-L. Lee, C.-Y. Lu, Y.-C. Lin and M.-R. Yang, *ECS Trans.,* 33(30) (2011) 39
10. A.L. Yerokhin, X. Nie, A. Leyland, A. Matthews and S.J. Dowey, *Surf. Coat. Tech.*, 122 (1999) 73
11. D.Q. Wei, Y. Zhou, D.C. Jia and Y.M. Wang, *Appl. Surf. Sci.,* 254 (2008) 1775
12. M. Wei, M. Uchida, H.M. Kim, T. Kokubo and T. Nakamura, *Biomaterials*, 23 (2002) 167
13. H. S. Ryu, W.-H. Song and S.-H. Hong, *Surf. Coat. Tech.*, 202 (2008) 1853
14. H.-J. Song, K.-H. Shin, M.-S. Kook, H.-K. Oh and Y.-J. Park, *Surf. Coat. Tech.*, 204 (14) (2010) 2273
15. H.P. Zhang, X.Y. Wang, S.J. Min, M. Mandal, M.Y. Yang and L.J. Zhu, *Ceram. Int.*, 40 (2014) 985

16. W.-H. Song, Y.-K. Jun, Y. Han and S.-H. Hong, *Biomaterials*, 25 (2004) 3341
17. M.-S. Kim, J.-J. Ryu and Y.-M. Sung, *Electrochem. Commun.*, 9 (2007) 1886
18. Y. Han, J. Sun and X. Huang, *Electrochem. Commun.*, 10 (2008) 510
19. S.H. Rhee and J. Tanaka, *Biomaterials*, 20 (1999) 2155
20. P. Kanchana and C. Sekar, *Mater. Sci. Eng. C-Mater. Biol. Appl.*, 42 (2014) 601
21. T. Dey, P. Roy, B. Fabry and P. Schmuki, *Acta Biomater.*, 7 (2011) 1873
22. T. A. Kuriakose, S. N. Kalkura, M. Palanichamy, D. Arivuoli, K. Dierks, G. Bocelli and C. Betzel, *J. Cryst. Growth*, 263 (2004) 517
23. L.-R. Chang, F.-H. Cao, J.-S. Cai, W.-J. Liu, Z. Zhang and J.-Q. Zhang, *Trans. Nonferrous Met. Soc. China*, 21 (2011) 307
24. S.V. Dorozhkin and M. Epple, *Angew. Chem.-Int. Edit.*, 41 (2002) 3130
25. H.-T. Chen, C.-J. Chung, T.-C. Yang, I-P. Chiang, C.-H. Tang, K.-C. Chen and J.-L. He, *Surf. Coat. Tech.*, 205(2010) 1624
26. S. Lebrette, C. Pagnoux and P. Aberlard, *J. Eur. Ceram. Soc.*, 26 (2006) 2727
27. Y. Han, S.-H. Hong and K. Xu, *Surf. Coat. Tech.*, 168 (2003) 249
28. W.-J. Zhu, Y.-J. Fang, H. Zheng, G.-X. Tan, H.-M. Cheng and C.-Y. Ning, *Thin Solid Films*, 544 (2013) 79
29. A. Lugovskoy and S. Lugovskoy, *Mater. Sci. Eng. C-Mater. Biol. Appl.*, 43 (2014) 527